3P5-10

Numerical model of contrast-enhanced ultrasound imaging coupled with nonlinear bubble dynamics

Junseok An[1†], Naohiro Sugita[2], and Tadahiko Shinshi[2] ([1]Dpt. Mech. Eng, Tokyo Tech; [2]FIRST, Tokyo Tech)

1. Introduction

Contrast-enhanced ultrasound (CE-US) is a type of medical ultrasound technology used to diagnose diseased organs and blood vessels with abnormal blood flow by increasing the image contrast using ultrasound contrast agents (UCAs) injected into the blood flow.

UCAs used in CE-US are gas-filled microbubbles (MBs) with a radius of 1-3 μm. MBs expand and contract in response to changes in surrounding pressure, and the volumetric oscillation generates strong scattered waves. The scattered waves from MBs exhibit nonlinear characteristics due to the compressibility of the internal gas, unlike the linear reflections from background tissue. CE-US employs nonlinear ultrasonic imaging techniques, such as pulse inversion (PI) and amplitude modulation (AM), to enhance the nonlinear components of the scattered waves while suppressing the linear components of the reflected waves[1]. However, even with the nonlinear ultrasonic imaging, the nonlinear components generated by the nonlinear acoustic propagation of the incident waves can still be transmitted to the tissue and included in the reflected waves.

In this research, the nonlinear oscillations of MBs, considering the nonlinear ultrasound waves from a ultrasound probe, are numerically computed. We aim to compare the advantages and limitations of nonlinear ultrasonic imaging techniques such as AM and PI through numerical simulation, and provide a new perspective on future nonlinear ultrasonic imaging techniques.

2. Numerical models

2.1 Propagation model of incident waves

The incident waves irradiated from a convex array probe propagate through the medium. In the ultrasound field, the waves in the compression phase propagate rapidly, while the waves in the expansion phase propagate more slowly. This spatial variation in propagation speed generates additional harmonics, and the sound pressure of the nonlinear harmonics depends on the nonlinear acoustic coefficient β. Given p_1 as the fundamental component of the incident pressure and p_2 as the second harmonics, with $p_1 \gg p_2$, the second harmonic component p_2 can be calculated using Burger's equation with the

E-mail: †an.j.ad@m.titech.ac.jp, *sugita.n.aa@m.titech.ac.jp

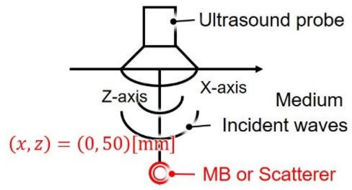

Fig. 1 Schematic representation of the simulation model consisting of a convex ultrasound probe, an isotropic medium, and point scatters (solid particles or MBs).

fundamental component p_1 as[2)]

$$(\nabla^2 + k^2)p_2 = -\frac{\beta k^2}{\rho_0 c_0^2} p_1 \tag{1}$$

where ∇ is the Laplacian, k is the wave number, c_0 is the speed of sound, and ρ_0 is the medium density. The fundamental component p_1 can be given using Garcia's medical ultrasound model[3)].

2.2 Dynamics model of MBs

The Rayleigh-Plesset equation coupled with Church's shell model describes the radial dynamics of an elastic spherical bubble as

$$\rho_0\left(R\ddot{R} + \frac{3}{2}\dot{R}^2\right) = P_G\left(\frac{R_0}{R}\right)^{3\kappa}\left(1 - \frac{3\kappa\dot{R}}{c_0}\right) - \frac{2}{R}\gamma(R) - \frac{4\dot{R}}{R^2}\kappa_s - 4\mu\frac{\dot{R}}{R} - p_0 + (p_1 + p_2) = 0 \tag{2}$$

where R and R_0 are the temporal and equilibrium bubble radii, P_G and p_0 are the equilibrium gas and the ambient pressure, κ is the polytropic index, γ and κ_s are the surface tension and viscosity of shell, μ is the effective viscosity.

2.3 Simulation model

Fig. 1 represents the probe' position and the location where the incident waves are measured. The probe used is a convex probe (Verasonics®, C5-2v) with 128 elements and a central frequency of 3.6 MHz, while the nonlinear acoustic coefficient β of the medium through which the sound waves propagate is 4.5. Also, by locating a scatterer with a scattering coefficient of 1×10^{-5} and a MB (GE healthcare®, Sonazoid) with a radius of 1.5 μm at the same position where the waves were measured, we calculate the reflected and scattered waves.

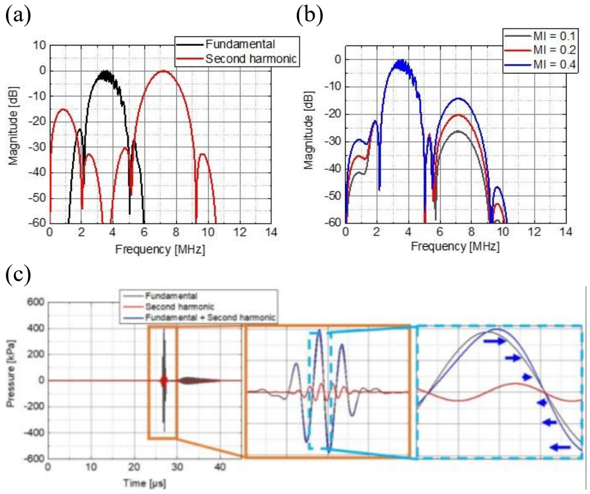

Fig. 2 (a) Frequency spectra of fundamental and second harmonic components and (b) the combined incident pressure for MI = 0.1, 0.2, 0.4. (c) The incident pressure waveform.

3. Results

3.1 Nonlinear propagation

Fig. 2 represents the frequency domain spectra and time domain pressure of the fundamental and second harmonic measured at $(x, z) = (0, 50)$ [mm] shown in **Fig. 1**. As shown in **Fig. 2(a)**, considering the nonlinear propagation, subharmonics and second harmonics of the fundamental frequency are generated. Also, these harmonics are amplified with increasing the mechanical index (MI) of the incident waves as depicted in **Fig. 2(b)**. Additionally, as illustrated in **Fig. 2(c)**, it is observed that the propagation of the high-pressure phase becomes faster, while the propagation of the low-pressure phase slows down.

3.2 Nonlinear ultrasonic imaging

Figs. 3(a-b) represent the results of applying AM to the reflected waves from a point scatterer and the scattered waves from a MB for MI = 0.1, 0.2, 0.4. **Figs. 3(c-d)** represent the results of applying PI. **Fig. 3(e)** summarizes the signal-to-noise ratio (SNR) and contrast-to-tissue ratio (CTR) obtained from the results in **Figs. 3(a-d)**. The SNRs were calculated by adding white noise to the ultrasound radio-frequency (RF) signals received by each element and then determining the relative intensity of MB to the noise in the ultrasound image. The CTRs were calculated as the ratio of the MB signal intensity to that of the point scatterer in the ultrasound images[4].

As shown in **Fig. 3(e)**, the AM exhibited low SNR and high CTR characteristics, while the PI showed high SNR and low CTR. Regardless of the methods, SNR improved with increasing in MI, while CTR improved with increasing MI in AM, indicating easier signal suppression from tissue. Also, it was observed that PI had an optimal MI.

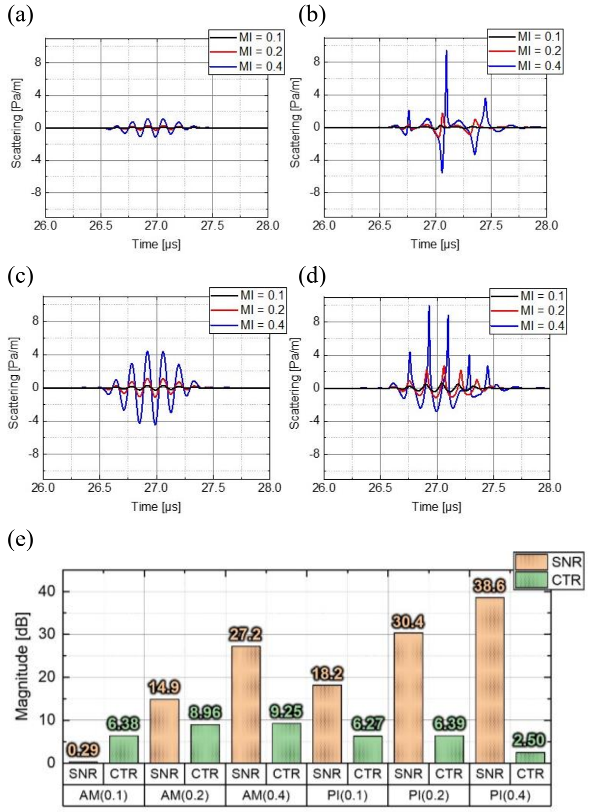

Fig. 3 (a, b) Reflected waves from a point scatterer and scattered waves from MB when applying AM, while (c, d) applying PI. (e) Comparison of SNR and CTR obtained by AM and PI.

4. Conclusion

We conducted CE-US imaging simulations utilizing the nonlinear oscillations of MB considering the nonlinear acoustic propagation. The AM exhibited characteristics of low SNR and high CTR, whereas the PI showed high SNR and low CTR. Furthermore, regardless of the methods, SNR improved with increasing MI. CTR improved with increasing MI in AM, and PI had an optimal MI for highest CTR. We expect that this proposed simulation will offer a new perspective for developing and evaluating new nonlinear ultrasonic imaging techniques in CE-US.

Acknowledgment

This work was supported by JSPS KAKEN Grant Number 23K13276.

References

1) T.-Y. Lai et al., IEEE Trans. Ultrason. Ferroelectr. Freq. Control, **68**, 5 (2021).
2) F. Varray et al., IEEE Trans. Ultrason. Ferroelectr. Freq. Control, **58**, 7 (2011).
3) D. Garcia, Comput. Meth. Prog. Bio., **218**, 106726 (2022).
4) H. Hu et al., 2015 IEEE Int. Ultrason. Symp., 2015, pp. 1-4.